



Synthesis, Characterisation and Electrochemical Studies of Cu (II) Complex of (E)-4-(2-(4-Methoxyphenyl) Diazenyl) Benzene 1, 3 Diol Including DNA Binding and Antibacterial Activity

Sukdev Maity¹, PK Saha² and Swapan Kumar Bhattacharya^{1*}

¹Department of Chemistry, Jadavpur University, Kolkata, West Bengal, India

²Department of Textile Technology, GCETTS, Hooghly, West Bengal, India

ABSTRACT

An innermetallic chelated azo-dye complex of second order having the stoichiometry $(Cu(L_1)_2, 2H_2O)$ with ligand L_1 , (E)-4-(2-(4-methoxyphenyl) diazenyl) benzene 1, 3 diol, has been synthesised at $pH = 7.48$ and studied in both solid state and aqueous phase using different spectroscopic techniques. The structure of the complex has been carried out from elemental analysis, UV-Vis, IR, and mass spectrophotometry. Thermal decomposition has been studied from TGA-DSC analysis. Cyclic voltammetry of the complex has been carried out to ensure the presence of Cu (II) in the complex $(Cu(L_1)_2, 2H_2O)$. Magnetic susceptibility determination of $(Cu(L_1)_2, 2H_2O)$ complex has been taken at a constant magnetic field of 5 KG with powder sample in the temperature range 20-35K. In addition special attention has been given to the studies of ct-DNA binding to the complex $(Cu(L_1)_2, 2H_2O)$ by absorption spectroscopy and cyclic voltammetry measurements under physiological condition ($pH=7.4, 25^\circ C$) with intrinsic binding constant in the order of $10^4 M^{-1}$. The complex also shows higher antibacterial activity than L_1 .

Keywords: Azo-dye Cu (II) complex; Antibacterial activity; Cyclic voltammetry; DNA binding; TGA; UV-visible

INTRODUCTION

A large number of azo-dyes have been synthesized recently and characterized by number of sophisticated spectroscopic methods. In addition, their wide ranges of analytical, industrial and biological applications have been shown earlier [1]. It is worth mentioning that these azo-dyes can function as good N, O donor chelating ligands and are so capable of forming a number of stable transition metal-azodye complexes both in solution phase and solid states (isolable) [2]. The characterizations of such complexes have also been successfully made [3]. But biological activities of such complexes are very limited. In this study we synthesis, characterization and biological activity of Cu (II) complexes have been reported. This paper also describe the structure elucidation of the Cu (II)- L_1 complexes using different techniques, where ligand L_1 is already reported [4,5]. The special attraction in the paper is the study of DNA interaction with Cu (II) azo dye complex [6,7]. Due to presence of azo-group (N=N) which along with some oxidisable functional groups like -OH, -OR, -NH₂ allow such compounds to interact with cells or DNA that may be probed to study such interaction in several biological activity or in medicine [8,9]. As many azo-dye compounds have been known to have general toxicity and carcinogenic in characteristics, transition metal azo-dye complexes have been shown to have significantly reduced toxicity as reported in many journals [10,11]. The present paper works with Cu (II) - L_1 complex who's binding with calf thymus deoxyribonucleic acid (CT DNA) is significant as considered from data collected from cyclic voltammetry and a series of UV-vis spectra of the complex of Cu (II) with L_1 . This study has attracted more attention because of their potential use as drugs, regulators of gene expression and tools for molecular biology [12]. These metal complexes are important as they may find their application as

antifungal, antibacterial, anti-convulsion, anti-inflammatory, anti-malarial, analgesic, platelets, anti-tuberculosis, anti-cancer activity. TGA of this complex has also been studied to predict relative thermal stability of the complex [13].

EXPERIMENTAL SECTION

All chemicals and solvents are of the highest purity taken from commercial suppliers such as Merck, BDH etc. and used without further purification. CuSO_4 (99.9% A.R, BDH) is the starting material for preparing $(\text{Cu}(\text{L}_1)_2 \cdot 2\text{H}_2\text{O})$ complex. Azo-dye ligand L_1 has been synthesized by previous method [4] and then recrystallised to get 99% of purity. Sodium acetate (anhydrous), triple distilled water, all are of analytical grade used for this purpose. For reference electrolyte used in cyclic voltammetry, phosphate buffer (pH=7.4) of A.R. quality has been used. CT DNA purchased from Sigma Chemical Company was dissolved in triple distilled water. Melting points of $(\text{Cu}(\text{L}_1)_2 \cdot 2\text{H}_2\text{O})$ complex was measured on electrically operated melting point apparatus of Sunder Industrial Products, Mumbai, India without calibration. The UV-Vis absorption spectrum was recorded using JASCO V-630 (UV-Vis) spectrophotometer in aqueous medium [3]. The infrared spectra were recorded on a Perkin-Elmer RX I FT-IR spectrophotometer with KBr discs ($4000\text{-}400\text{ cm}^{-1}$). Elemental analysis (C, H, N, O) was carried out using a Perkin-Elmer 2400 II elemental analyser. Cyclic voltammetry experiments were performed using model no. DY2300 series potentiostat, Digi-IVY Instrument, SDT Q600 V8.2 Build 100 was used for the analysis of TGA-DSC.

Synthesis of $\text{Cu}(\text{L}_1)_2$ Complex

CuSO_4 is collected and dissolved in 100 ml triple distilled water to get a solution of 0.1(M). To this solution is added saturated solution of L_1 in methanol such that $\text{Cu}(\text{II})\text{:L}_1$ is 1:2 in molar ratio. The mixture is then taken in a well stoppered conical flask which is then agitated by a magnetic stirrer followed by addition of saturated solution of sodium acetate and heating at constant temperature of 50°C for 2 hour. The mixture is then filtered under suction pump. The black brown solid is repeatedly washed by methanol-water mixture till the filtrate is almost colour-less [6]. The deep brown residue is then re-crystallised.

RESULTS AND DISCUSSION

Physical Properties and Elemental Analysis

Physical properties and elemental analysis (C,H,N,O) of $\text{Cu}(\text{II})\text{L}_1$ complex are recorded in Table 1. A single spot is located in the TLC, which suggests high purity of the complex. It is also supported by a low percent error (with in 5%) in elemental analysis in Table 2 and sharp decomposition temperature determined from TGA-DSC [13-15].

Table 1: Some physical properties of synthesized complex $\text{Cu}(\text{L}_1)_2$

Name of complex	Empirical formula	Relative molar mass Found(Calc.)	R _f value	pH	Colour	M.P (°C)
$\text{Cu}(\text{L}_1)_2 \cdot 2\text{H}_2\text{O}$	$\text{Cu}(\text{C}_{13}\text{H}_{11}\text{N}_2\text{O}_3)_2 \cdot 2\text{H}_2\text{O}$	585.50(589.26)	0.71	6.52	Black brown	284

Table 2: Elemental analysis of synthesized complex $\text{Cu}(\text{L}_1)_2$

Name of complex	yield %	Carbon % Found(Calc.)	Hydrogen% Found(Calc.)	Nitrogen% Found(Calc.)	Oxygen% Found(Calc.)	Copper% Found(Calc.)
$\text{Cu}(\text{L}_1)_2 \cdot 2\text{H}_2\text{O}$	71	53.49(53.28)	3.80(3.76)	11.42(9.56)	21.40(21.52)	10.82(10.86)

Electronic Spectrum of the Complex (UV-Vis)

The UV-vis spectra for $(\text{Cu}(\text{L}_1)_2 \cdot 2\text{H}_2\text{O})$ has been recorded in (i) aqueous Solution (10^{-5}M) and (ii) phosphate buffer, pH=7.4 (10^{-3}M). From Electronic spectra (UV-Vis) it is speculated that majority of mono nuclear $\text{Cu}(\text{II})$ complexes are either square planar or highly distorted octahedral in nature. This ligand being a chelated N,O donor ligand (azo-N and phenolic O) demands that it might form a stable bis- $\text{Cu}(\text{II})$ chelate internally compensated with or without axially populated by two H_2O molecules, which might be thought to be a distorted octahedral complexes [16-20]. So $(\text{Cu}(\text{L}_1)_2(\text{H}_2\text{O})_2)$ will show a $\text{Cu}(\text{N}_2\text{O}_2)$ chromophores. This will give rise to UV-Vis spectrum which exhibited $n \rightarrow \pi^*$ or $\pi \rightarrow \pi^*$ charge transfer band at 420 nm. There will be another broad band observed at 381nm and 254 nm which is attributed to d-d transition [21,22]. The experimentally obtained absorption spectrum (UV-Vis) are graphically represented in Figure 1.

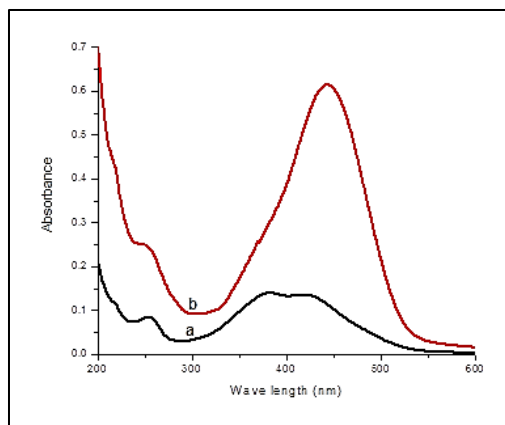


Figure 1: UV-Vis of the Cu(II) complex in (a) aqueous Solution and (b) buffer solution

The peaks obtained from aqueous solution are (i) $\nu_1 = 23809 \text{ cm}^{-1}$, corresponds to the transition ${}^2B_{1g} \rightarrow {}^2B_{2g}$, (ii) $\nu_2 = 26246 \text{ cm}^{-1}$, corresponds to the transition ${}^2B_{1g} \rightarrow {}^2A_{1g}$, (iii) $\nu_3 = 39370 \text{ cm}^{-1}$ corresponds to the transition ${}^2B_{1g} \rightarrow {}^2E_g$

All these are d-d bands where the tail of the blue ends shows a shift to reddish brown [11]. The formations of three peaks is attributed to anticipated distorted octahedral ligand field (JahnTeller distortion).

The bands appearing in the UV-Vis spectra of Cu(II) complex in phosphate buffer solution is comparable to that recorded in aqueous solution expect the missing of the peak at 420 nm in buffer solution and shifting of the peak at 381 nm is shifted to 443 nm that is towards the blue region. At the alkaline pH (phosphate buffer solution 7.4) there is some chances of producing anionic complex or axial H_2O might be replaced by HPO_4^{2-} ion and intra ligand charge transfer band at 420 nm may merge with the band at 443 nm (d-d).

Infrared Spectra

IR- spectrum of L_1 has already been reported [4], where strong bands around 1246.75 cm^{-1} , 1177.33 cm^{-1} , 1107 cm^{-1} and 1025.94 cm^{-1} have appeared in conformation with the characteristic band for C-O stretching as mixed band of alkyl C-O and aryl C-O stretching [23]. In the IR spectrum of the complex these bands remain unaffected as shown in the Figure 2, which appear around 1249.65 cm^{-1} , 1187.94 cm^{-1} , 1109.83 cm^{-1} and 1026.91 cm^{-1} respectively. By comparing with L_1 it is also suggested that free OH band at 3753.64 cm^{-1} is a weak stretching band and H-bonded OH band at 3456.82 cm^{-1} is a broad band, are almost missing or appear as very weak bands with high %T, as presented in the Figure 2 in this complex. It means that one phenolic 'O' is attached to Cu(II) which corresponds to stretching at 519.72 cm^{-1} . There is another bonding Cu-N whose stretching occur at 442.58 cm^{-1} . It is known that the ligand L_1 is an unsymmetrical ether ($\text{CH}_3\text{-O-Ar}$), So the two C-O bond coupled to give anti symmetrical and symmetrical C-O stretching absorption for three different IR bands appeared and already mentioned earlier. The bands appearing at 1460.81 cm^{-1} and 1361.5 cm^{-1} are distinctly less intense than that obtained in free ligand L_1 in bending frequency of $\nu_{\text{N=N}}$. This lowering in stretching of azo group might correspond to partial drifting of the π -electron cloud towards metal in addition to Cu(II)-N σ -bonding. Consequently N-N bond order decreases and finally it assumes an approximate Cu(II)-N (=N) σ -bonding might go into partial chelation (haptacity). Linear stretching of N=N is absent as it is IR inactive (Figure 2). The band appearing between 1500 cm^{-1} - 1600 cm^{-1} (1595.81 cm^{-1} , 1505.17 cm^{-1} and %T=30.5732 and 48.8876) obviously indicate C=C (aromatic) bonding which is not appeared in complex [24]. Band offering at 2939.95 cm^{-1} is very close to Ar-H bonding of theoretically known to be 3030 cm^{-1} .

Mass Spectral Studies

It is predicted from C,H,N analysis that molecular formula of Cu(II) L_1 complex is $(\text{Cu}(L_1)_2 \cdot 2\text{H}_2\text{O})$ This formula having relative molar mass 585.5 is roughly in agreement with m/z peak at 588.16, a value having 0.6% error might be due to adhering moisture. This complex is primarily considered to an internally compensated with L_1 anions in a square planer ligand field as observed from analysis of number of square planer Cu(II) complex with $\text{Cu}(\text{N}_2\text{O}_2)$ chromophores [11]. Two water molecules may have two different attachments that either two axial sites are occupied by two H_2O molecules or two H_2O molecules may be H-bonded with free phenolic -OH groups.

Another (m/z) peak appearing at 610.76 might appear due to knocking out H_2O molecules and attachment of OAc^- . The impurity OAc^- comes from the NaAc soln. which was used during synthesis of the complex. The composition

(Cu (L₁)₂(OAc)₂)⁻² can not be ruled out as Cu⁺² may have an affinity towards OAc⁻ and the peak m/z appearing at 668.71 which is the calculated Value of mass as 667.57 the nearby pecks at 662.72, 664.79, 661.69 might be generated by loss H⁺ from the complex successively [25,26]. The high peak m/z appearing at 706.26 should indicate the stoichiometr (Cu (L₁)₂(OAc)₂), 2H₂O, due to presence of two H₂O molecules as water of crystallization. Attachment of H₂O to H-bonding with free phenolic OH or axially located H₂O is not unlikely (Figure 3). Loss of one H₂O is possible, which causes another peak characterized by m/z at 688 very close to actually observed peak at 684.29 [27].

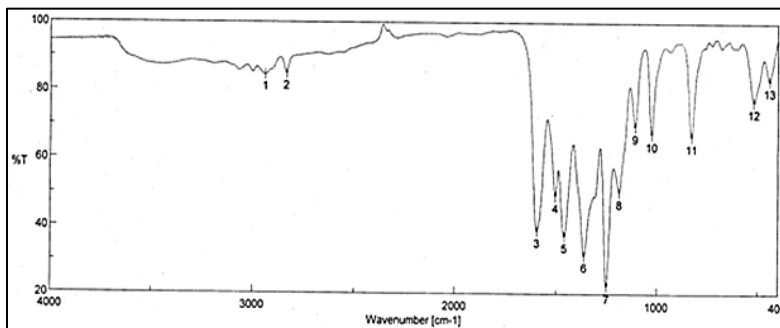


Figure 2: IR spectrum of Cu(II) complex

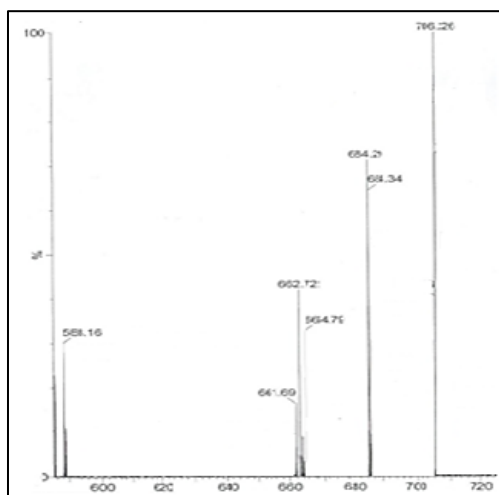


Figure 3: Mass spectra of sodium salt of Cu(II) complex

TGA-DSC Studies

The thermo gravimetric analysis (Figure 4) gives information about the thermal stability of the complex and suggests a general scheme for thermal decomposition of the Cu(II) chelate complex. In the present investigation, heating rates were suitably controlled at 10°C min⁻¹ under nitrogen atmosphere [12,13,17]. The thermo gram of the Cu (II) complex shows three decomposition steps (Table 3) within the temperature range 25-294°C. The first step involves loss of non-co-ordinated water molecules around 60-106°C with an estimated mass loss 6.53% (calculated mass loss 7.21%), the second step involves loss of two co-ordinated water molecules around 106 - 208°C with an estimated mass loss 12.19% (calculated mass loss 10.32%) and the third step involves loss of one molecule of ligand around 208-294°C with an estimated mass loss 27.46% (calculated mass loss 27.71%). This thermo gram is (Figure 4) accompanied by three exothermic peak at 103°C, 190°C, 207°C and 243°C on the DSC curve [18].

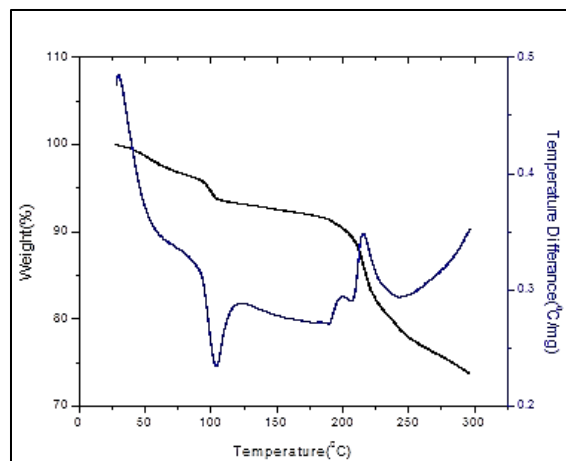


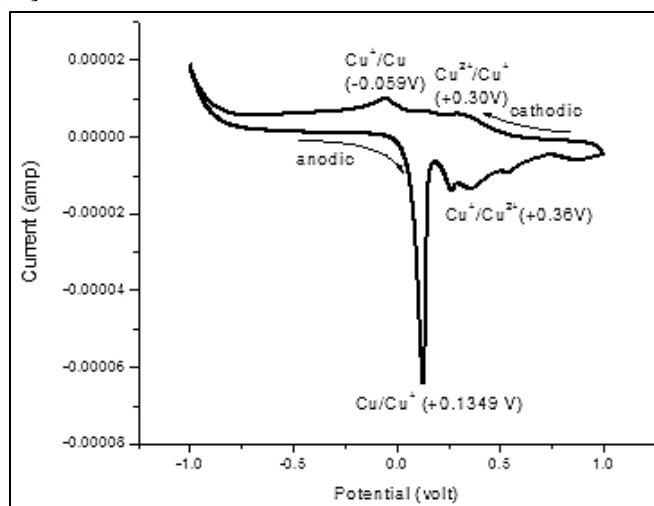
Figure 4: TGA and DSC curve of Cu(II) complex

Table 3: Thermal analytical results (TGA, DSC) and micro analytical data of complex

Metal Complex	TGA Range(°C)	Mass loss % Estim.(Calc.)	Assignment	DSC Peak (°C)	Molar Conductivity (S.cm ² .mole ⁻¹)	μ_{eff} B.M
Cu(L ₁) ₂ .2H ₂ O	60-106	6.53 (7.21)	Moisture	103	384.07	1.93
	106-207	12.19 (10.32)	Co-ordinated Water loss	190, 207		
	207-294	27.46(27.71)	Loss of one ligand	243		

Electrochemical Studies of Cu (II) Complex with L₁

Cyclic voltammetry experiments were performed using model number DY2300 series potentiostat, Digi-IVY. The experiments were carried out using the conventional three-electrode system at 25°C. A Pt disc electrode served as the working electrode A calomel electrode Saturated with KCl was used as reference electrode while a platinum wire served as the counter electrode. Electrochemical measurements were performed in a 10 mL electrochemical cell. 5×10^{-3} (M) metal complex solution was prepared using phosphate buffer (pH=7.4) solution which was used as supporting electrolyte [1,3,14].

Figure 5: Cyclic voltammogram of (Cu(L₁)₂.2H₂O) complex is recorded using platinum electrode at scan rate 50 mVs⁻¹

The Cu(II) complex of L₁ showed two reduction (cathodic) peaks at +0.30 V (Cu²⁺/Cu⁺) and -0.059V (Cu⁺/Cu) respectively in the Figure 5. For the Cu(II)L₁ complex the first reduction was attributed to reduction of Cu²⁺ + e → Cu⁺ due to single electron gain, while the second reduction was of Cu⁺ + e → Cu due to another single electron gain. In addition to these two reduction (cathode) peaks for the complex, there was one very sharp oxidation (anodic) peak at +0.135 V which was due to generation of Cu/Cu⁺ species and another peak at +0.36 V due to conversion of Cu⁺ - e → Cu²⁺. This was supported by a recent finding where an almost identical condition was used for a Cu(I) complex

[6,8]. Plot of anodic peak current I_{pa} with square root of scan rate ($v^{1/2}$) being linear, the oxidation for Cu(I) complex (Figure 2) indicate a diffusion controlled process with no adsorption on the electrode surface [11].

DNA Binding Studies

Absorption spectral measurements:

All experiments involving calf thymus DNA (CT- DNA) were performed in Tris- buffer solution (50 mM NaCl/5 mM Tris-HCl, pH 7.4) at $25 \pm 0.2^\circ\text{C}$. Double distilled water was used to prepare the buffer solution. The concentration of CT- DNA was determined from the intensity of absorbance at 260 nm with a known extinction coefficient value ($\epsilon_{260}=6600 \text{ M}^{-1} \text{ cm}^{-1}$) [1]. The ratio of the absorbance of CT DNA at 260 nm and 280 nm was found as 1.85. Therefore, no further purification was attempted [6]. Absorption titration measurements were carried out by varying the concentration of CT DNA from 0 to $10 \times 10^{-6} \text{ M}$, while keeping the metal complex concentration constant at $12 \times 10^{-6} \text{ M}$. Samples were incubated at $25 \pm 0.2^\circ\text{C}$ for 24 hour before recording each spectrum (Figure 6). The intrinsic binding constant (K_b) for the interaction of the complex with ctDNA was determined using the following equation [11].

$$(\text{DNA})/(\epsilon_a - \epsilon_f) = (\text{DNA})/(\epsilon_b - \epsilon_f) + 1/K_b(\epsilon_b - \epsilon_f) \quad (1)$$

where (DNA) is the concentration of CT DNA, the apparent absorption coefficients ϵ_a , ϵ_f and ϵ_b correspond to $A_{\text{obsd}}/(\text{Cu})$, the extinction coefficient for the free Cu(I) complex and the extinction coefficient for the Cu(II) complex in the fully bound form, respectively. A plot of $(\text{DNA})/(\epsilon_a - \epsilon_f)$ vs (DNA) gave a slope of $1/(\epsilon_b - \epsilon_f)$ and a Y-intercept, $1/K_b(\epsilon_b - \epsilon_f)$, K_b is the ratio of the slope to the Y-intercept (Figure 7). The absorption spectra of the complex in the absence and presence of increasing amounts of CT-DNA concentration are shown in Figure 6. With increasing concentrations of DNA, the complex exhibited hypochromism with slight red shifts of the absorption bands at 443 nm observed in the presence of DNA can be assigned to LMCT transitions in the absorption spectra of all complexes. The changes in the absorbance values with increasing amounts of CT DNA were used to evaluate the intrinsic binding constant K_b . Based on the hypochromism exhibited and shifts in absorbance upon addition of CT DNA, non-intercalative interaction probably by an electrostatic interaction between complex ions and negatively charge phosphate groups of the CT DNA can be predicted [6]. However, since DNA possesses several hydrogen bonding sites which are accessible both in the minor and major grooves, a favorable hydrogen bonding may be formed between the coordinated and non-coordinated amine -NH- groups of the complex with the base pairs in CT DNA. Further, the intrinsic binding constant (K_b) of the complex calculated by using Eq. (1) is found to be $1.69 \times 10^4 \text{ M}^{-1}$.

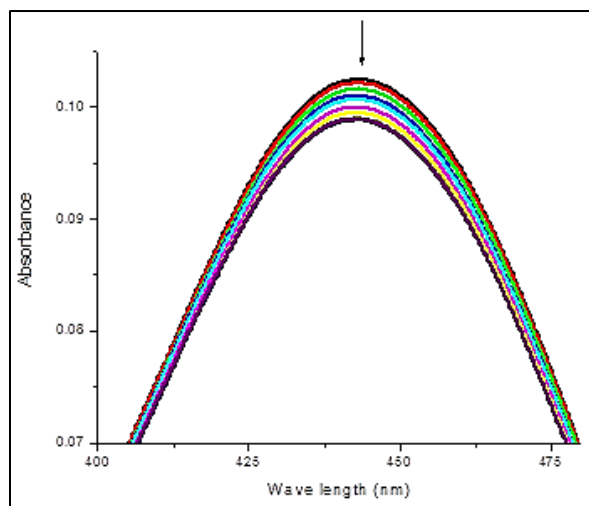


Figure 6: Absorption spectra of Cu(II) complex in the absence and in the presence of increasing concentration of CT DNA; the top most spectrum is recorded in the absence of DNA and spectra below on successive addition of 1 μl DNA to it

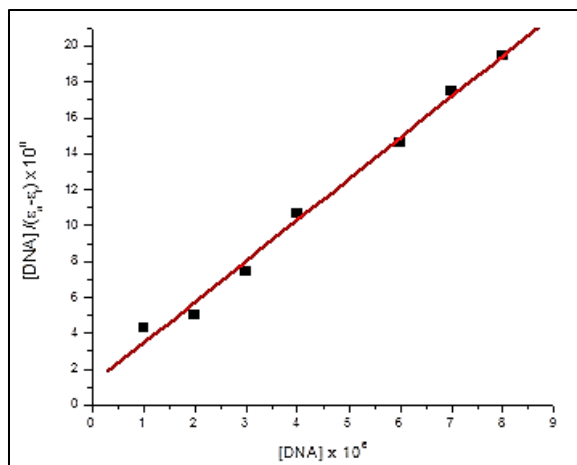


Figure 7: A plot of $(DNA)/(\epsilon_a - \epsilon_f)$ vs. (DNA)

The data obtained from the spectrophotometric titration of Cu(II) complex with ct DNA was analyzed by Scatchard plot [1]. The intrinsic binding constant (K') and site size (n_b) were determined directly using eqn. (5):

$$\frac{r}{c_f} = K' (n - r) \quad (5)$$

$r = C_b/C_D$ where ' C_b ' is the concentration of bound compound and ' C_D ' concentration of ct DNA ' C_f ' refers to the concentration of free compounds. K' is (1.74×10^4) the intrinsic or the overall binding constant of any molecule with a substrate. ' n ' is (3.5) the binding stoichiometry in terms of number of bound compound (Cu(II) complex) per nucleotide while ' n_b ' is (0.28) the reciprocal of ' n ' i.e., the binding site size in terms of number of nucleotide per molecule of the compounds that were used. The overall binding constant K' is also related to K_{app} by $K' = K_{app} \times n_b$ [1]. Therefore knowing n_b and using the K_{app} values the intrinsic binding constant K' could be evaluated for the interaction of the Cu(II) complex with ct DNA. The K' values obtained in this manner for complex was compared with values obtained directly from Scatchard plots (Figure 8). Thus using different modes of evaluation both apparent binding constant (K_{app}) and intrinsic binding constant (K') were obtained from where an idea of the strength of interaction of the Cu(II) complex with ct DNA could be obtained.

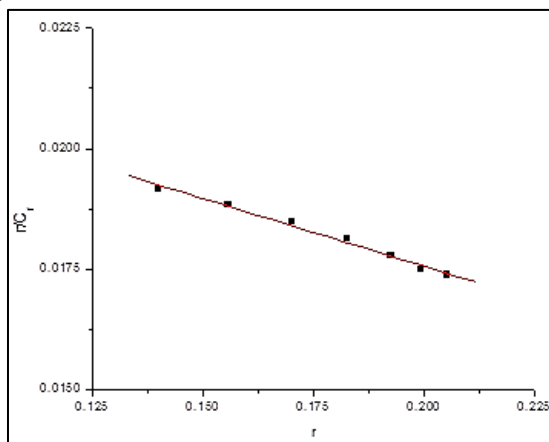


Figure 8: Scatchard plot obtained from the spectrophotometric titration of Cu(L1)2.2H₂O with CT DNA

Cyclic voltammetric measurements:

The voltammogram of Cu(II) azo-dye complex showed steady redox peaks in the potential range of +1.0 to -1.0 V in either scan i.e., in forward scan anodic peak and in reverse scan cathodic peak appeared [6]. This cyclic voltammogram of Cu(II) azo-dye complex showed one electron transfer and the reaction is totally reversible electrochemical reaction. By mixing 30, 60, 90, 120 and 150 μ M CT-DNA into 2 mM Cu(II) azo-dye complex solution (Figure 9) the change in peak potential and decrease in current i_{pa} was being seen. The decrease in peak current i_{pa} is due to diffusion of Complex into double helix DNA which resulted supramolecular complex formation, due to which transfer of electrons was being reduced as a result number of free molecules was being

decreased. The change in value of formal potential explained the nature of binding between Cu(II) azo-dye complex and DNA. Generally intercalation of small molecules into double helical deoxyribonucleic acid caused positive change in the peak potential, whereas negative change revealed binding of the positively charged molecule with the negatively charged phosphate, $(\text{PO}_4)^{-3}$ moiety present on DNA backbone called the electrostatic interaction [8]. The negative change in peak potential was observed for Cu(II) azo-dye complex by the addition of different concentration of CT-DNA, revealed the electrostatic nature of interaction. The binding constant can be calculated by using following equation; $\{1/(\text{DNA}) = K(1-A)/1-(i/i_0) - K\}$, where i_0 and i are the peak currents in absence and presence of CT-DNA, K is the binding constant, and A is the proportionality constant. If we plot a graph between $1/(\text{DNA})$ and $1/(1-i/i_0)$, binding constant (K) can be calculated which was $2.02 \times 10^4 \text{ M}^{-1}$ (Figures 10 and 11). The changed binding free energy $(-\Delta G = RT \ln K \text{ at } 25^\circ\text{C})$ of compound Cu(II) azo-dye complex was calculated to be $30.25 \text{ kJ mol}^{-1}$ exhibited the spontaneity of Cu(II) azo-dye complex -DNA interaction.

The diffusion coefficient of free compounds and compound-DNA adduct was calculated from Randles-Sevcik equation; $(I_{pa} = 2.69 \times 10^5 n^{3/2} A C_0^* D_0^{1/2} v^{1/2})$ where I_{pa} is referred to anodic peak current in ampere, v referred as scan rate in V s^{-1} , C_0^* is concentration in mol cm^{-3} , A is cross sectional area of electrode in cm^2 , n is number of electrons involved in the reaction, D_0 is diffusion coefficient in $\text{cm}^2 \text{ s}^{-1}$. The diffusion coefficient of free Cu(II) azo-dye complex was calculated 4.609×10^{-3} whereas diffusion coefficient of Cu(II) azo-dye complex -DNA was found to less i.e., 1.918×10^{-3} . The decreased diffusion coefficient value for Cu(II) azo-dye complex -DNA adduct can be justified as free molecules are easy to diffuse and is of low molecular weight so exhibit more peak current whereas when compound Cu(II) azo-dye complex was interacted with DNA, the quantity of free molecules became less with the obvious a result of decrease in current.

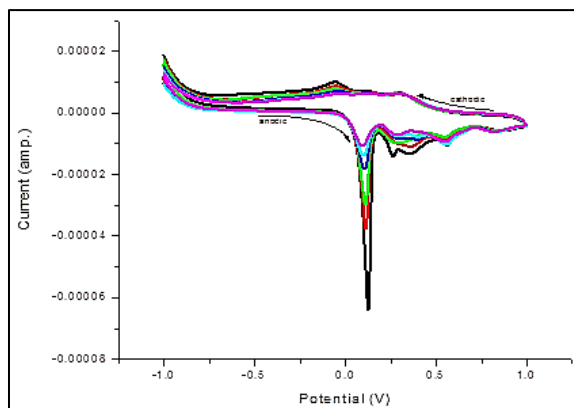


Figure 9: Cyclic voltammograms of 2 mM Cu(II) azo-dye complex in the absence and presence of 30 μM , 60 μM , 90 μM , 120 μM and 150 μM DNA showing a decrease in I from I_0 and a -ve shift in peak potential indicating electrostatic interactions

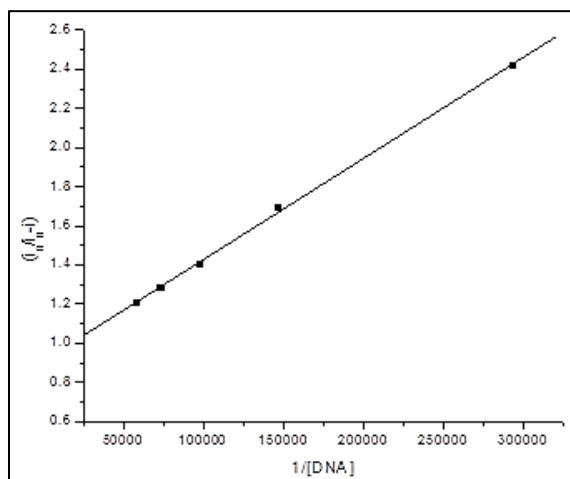


Figure 10: The plot of (i_0/i_0-i) vs $1/[\text{DNA}]$ for determination of binding constant

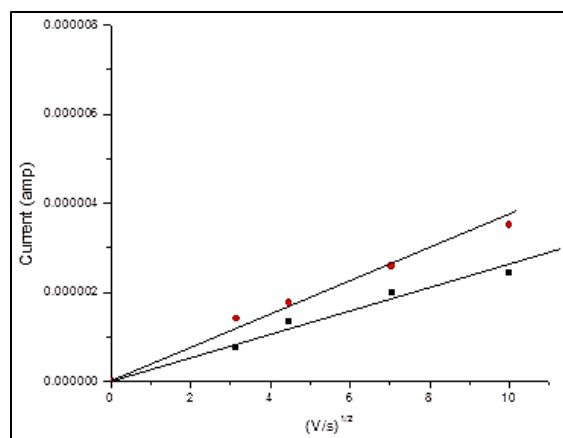


Figure 11: The plot of $I_{pa} vs v^{1/2}$ (square root of scan rate) for the determination of diffusion co-efficients of $(Cu(L_1)_2 \cdot 2H_2O)$ complex ($0 \mu M$ ct DNA) and $(Cu(L_1)_2 \cdot 2H_2O)$ -DNA in phosphate buffer (pH=7.4) as solvent

Antibacterial activity:

The Cu(II) complex was tested against the bacteria *Escherichia coli*, *Bacillus subtilis*, *Staphylococcus aureus*, *Swmonellatyphi*. Diameter of incubation zone: 15 mm, concentration of bacterial growth $200 \mu g/mL$, in DMSO solution (-) : Inactive. The data in the Table 4, it is observed that the Cu(II) complex is more active against all the test organisms, *Bacillus subtilis* and *Staphylococcus aureus* and as well as more active compared to the L_1 . Such increased activity of the Cu(II) complex can be explained with respect to Overtone's concept and Tweedy's chelation theory [8]. According to Overtone's concept of cell permeability, the lipid membrane that surrounds the cell favours the passage of only the lipid-soluble materials whose liposolubility is an important factor, which controls the antibacterial activity. On chelation, the polarity of the Cu(II) ion is reduced [6,12] to a great extent due to the overlap of the ligand, L_1 orbital and partial sharing of the positive charge of the Cu(II) ion with donor groups. On the other hand it increases the delocalization of π electrons over the whole chelate ring and enhances the lipophilicity of the Cu(II) complex. This increased lipophilicity enhances the penetration of the Cu(II) complex into lipid membranes and blocking of the cobalt metal binding sites in the enzymes of micro-organisms. This Cu(II) complex also disturb the respiration process of the cell and thus block the synthesis of proteins, which restricts further growth of the organisms.

Table 4: Antibacterial activity of Cu(II) complex

Metal Complex	Rate of oxidation (Antibacterial activity)				
	Control	Swmonellatyphi	Staphylococcus aureus	Escherichia coli	Bacillus Subtilis
$Cu(L_1)_2 \cdot 2H_2O$	7	13	11	15	17

CONCLUSION

The complex of Cu(II) azo-dye has been synthesized and structure of the complex has been established by elemental analysis, IR, electronic, mass spectroscopy, molar conductance. Electronic spectral data suggest that the complex has distorted octahedral geometry. The complex exhibits good redox property. The complex had shown significant binding with CT-DNA by non-intercalative mode i.e., Electrostatic interactions. The complex act as potent bactericidal agent. Further work with analogs is needed.

ACKNOWLEDGEMENT

This work has been funded by Jadavpur University in the form of a "J.U Research Grant" to Prof. Dr. Swapan Kumar Bhattacharya, Department of Chemistry, Jadavpur University. The authors are thankful to the authorities of Chemistry Department of Jadavpur University and Department of Textile Technology, GCETTS, HOOGHLY for allowing them to pursue this research work.

REFERENCES

- [1] T Deb; D Choudhury; PS Guin; MB Saha; G Chakrabarti; S Das. *Chem Biological Interact.* **2011**, 189, 206-214.
- [2] T Dev; S Khamrai; PS Guin; MB Saha; PC Mandal; S Das. *Int J Pure Appl Chem.* **2009**, 4, 131-137.
- [3] S Maity; PK Saha; SK Bhattacharya. *IOSR J Appl Chem (IOSR-JAC).* **2016**, 9(9), 1-10.
- [4] S Maity; A Chakraborty; PK Saha; MB Saha; SK Bhattacharya. *J Indian Chem Soc.* **2015**, 92, 43-50.
- [5] PK Saha; MB Saha. *J Indian Chem Soc.* **1995**, 72, 755-758.
- [6] A Bimolini Devi; N Rajen Sing; M Damayanti Devi. *J Chem Pharm Res.* **2011**, 3(6), 789-798.
- [7] K Pandey; P Giri; R Patra; SK Bhattacharya; MB Saha. *J Indian Chem Soc.* **2007**, 84, 256-258.
- [8] B Lal; S Aktar; AA Altaf; A Badshah; RA Hussain; H Li. *Int J Electrochem Sci.* **2016**, 11, 1632-1639.
- [9] Anitha; KR Venugopala; VKS Rao. *J Chem Pharm Res.* **2011**, 3(3), 511-519.
- [10] VA Modhavadiya. *Asian J Biochem Pharm Res.* **2015**, 5(3), 131-135.
- [11] M Swetha; A Suseelamma. *European J Biomed Pharm Sci.* **2016**, 3(4), 260-264.
- [12] SJ Kirubavathy; R Velmurugan; K Parameswar; S Chitra. *Arabian J Chem.* **2014**, 1-6.
- [13] HA Habeeb; JA Khalid; AJ Suadada. *Oriental J Chem.* **2015**, 31(2), 809-818.
- [14] S Ershad; J Khodmarz. *Int J Electrochem Sci.* **2010**, 5, 1302-1309.
- [15] A Chakraborty; PK Saha; C Dutta; AR Das; MB Saha. *Colourage.* **2009**, 7, 2-86.
- [16] YB Taura; SM Gumel; S Habibu; JL Adam. *IOSR J Appl Chem (IOSR-JAC).* **2014**, 7(8), 34-37.
- [17] S Wang; S Shen; H Xu. *Dyes Pigments.* **2000**, **441**, 95-198.
- [18] D Canakci; OY Saribiyik; S Serin. *Int J Sci Res Innovative Technol.* **2014**, 1(2), 52-72.
- [19] A Perveen; T Nezamoleslam; II Naqvi. *African J Pure Appl Chem.* **2013**, 27(6), 18-224.
- [20] H Khanmohammadi; M Darvishpour. *Dyes Pigments.* **2009**, 81, 167-173.
- [21] D Banerjea. *Co-Ordination Chemistry*, Second Edition, Asian Books Private Limited, **2010**.
- [22] E James; AK Ellen; LK Richard; KM Okhil. *Inorganic Chemistry, Principles of Structure and Reactivity*, Second Impression, Pearson Education, **2007**, 473-474.
- [23] RL Dutta, A Shyamal. *Elements of Magneto Chemistry*, 2nd edition, Affiliated East-West press Pvt. Ltd. (EWP), 103, **1993**.
- [24] William Kemp. *Organic spectroscopy*, 3rd Edition, Palgrave, New York, **1991**.
- [25] MS Robert; WX Francis. *Spectrometric Identification of Organic Compounds*, Sixth Edition, John Wiley & Sons, Inc. New York, **1996**.
- [26] RD John. *Application of Absorption Spectroscopy of Organic Compounds*. 6th edition, P.37, **1987**.
- [27] D Nicholas. *Pergamon Texts in Inorganic Chemistry*. Pergamon Press Oxford. 1st edition, **1973**.